Designing Robust Air Transportation Networks via Minimizing Total Effective Resistance

Changpeng Yang, Jianfeng Mao, Xiongwen Qian, Peng Wei

***Abstract*—Designing a robust air transportation network is an ongoing research effort that seeks to improve the extent of a network being connected against failures and attacks. The total effective resistance can be a promising measure for network robustness as demonstrated by case studies conducted in this paper. To enhance the robustness of air transportation networks, we consider to solve a flight route selection problem, in which a set of routes are chosen from a candidate route set to minimize the utility function defined by the total effective resistance. Since it is an integer nonlinear programming problem, to balance the trade-off between optimality performance and computational efficiency, two methods that implement the total effective resistance are developed to suit different network scales. For small/medium-scale networks, we develop an interior-point method based on convex relaxation and duality gap, which achieves a near optimality performance within acceptable time. For large-scale networks, we develop an accelerated greedy algorithm based on proved monotone submodularity, which can substantially reduce the computation time in deriving a good solution with a guaranteed optimality gap. Their optimality performance and computational efficiency are verified and compared through numerical results. Moreover, three case studies from real world examples are also performed to demonstrate the application of the proposed methods for different network scales.**

***Index Terms*—Air Transportation Network, Total Effective Resistance, Route Selection, Convex Relaxation, Submodular.**

I. INTRODUCTION

THE past decade has witnessed the rapid development of emerging discipline of network science for applications in air transportation networks [1], [2]. An air transportation network can be viewed as a weighted graph $G(V, E, W)$, where the node set V represents airports, the edge set E represents flight routes between nodes and W denotes edge weights encoding edge information, such as flight cancellation rates and numbers of flights [3]. As shown in the OpenFlights Database 2012 [4], about 99.44% (36002/36203) flight routes in the global air transport network are bidirectional and one-way routes usually exist between small cities. Moreover, it is more beneficial to improve the robustness of the network of critical hubs, which are all connected by bidirectional routes. Hence, we model air transportation networks as undirected graphs.

The studies of air transportation networks mainly focus on the analysis of the underlying structural characteristics, the functional characteristics, and the network dynamics. Nowadays, flight delays and cancellations are more and more common. The US national on-time arrival performance during 2016 is 81.42%, 17.41% of flights are delayed for more than 15 minutes, and the rest 1.17% are canceled [5]. These delayed or canceled flights are caused by various types of natural and/or man-made disruptions on edges or nodes. The disruptions include severe weather, mechanical failures, demand limiting, long airspace flow program, flight delay/cancellation and other unforeseen events [5]. An important issue in air transportation networks is to design a network to be robust to disruptive incidents that greatly affect or interrupt aviation activities [6]. Structural robustness, the basis of the error tolerance of the complex systems, is one of the most fundamental characteristics representing how a network maintains its function under disruptive events [7], [8]. More specifically, an air transportation network with high robustness should be capable of mitigating the impacts of possible failures of nodes or edges.

In this paper, we concentrate on improving the structural robustness of the air transportation network. Similar to the difficulties encountered in the integrated systems with large-scale networks [9], it is critical to address how to fairly evaluate the structural robustness of air transportation networks. To the best of our knowledge, there is no standard answer to this question. In the literature, many efforts have been made to measure and evaluate the robustness of air transportation network in terms of connectivity, betweenness centrality, degree centrality, eigenvector centrality, and clustering coefficient [10], [11], [12], [13]. Although these metrics are good to reveal some local or global topology characteristics of air transportation network robustness, they have some drawbacks in optimizing network robustness. For example, since betweenness centrality only takes into account the shortest paths between nodes without considering alternative paths, it may not be able to fully capture network structural robustness. And the measures of edge connectivity and vertex connectivity may be

C. Yang was with the School of Mechanical and Aerospace Engineering, Air Traffic Management Research Institute, Nanyang Technological University, 639798, Singapore (cyang008@e.ntu.edu.sg). He was also affiliated with UC Berkeley NEXTOR II, Berkeley, CA 94720, USA (chpyang@berkeley.edu). Now he is a senior operations researcher in SF express (changpengyang@sf-express.com)

J. Mao is with the School of Science and Engineering, Shenzhen Key Laboratory of IoT Intelligent Systems and Wireless Network Technology, The Chinese University of Hong Kong, Shenzhen, Guangdong, 518172, P.R. China (jfmao@cuhk.edu.cn).

X. Qian is with the School of Mechanical and Aerospace Engineering, Air Traffic Management Research Institute, Nanyang Technological University, 639798, Singapore (xqian003@e.ntu.edu.sg).

P. Wei is with the Department of Aerospace Engineering, Iowa State University, Ames, IA 50011 (pwei@iastate.edu).

The authors' work is supported in part by National Natural Science Foundation of China under grant U1733102, by Shenzhen Science and Technology Innovation Committee under grant ZDSYS20170725140921348, by CUHKSZ under grant PF.01.000404, by the Air Traffic Management Research Institute, NTU and the Civil Aviation Authority of Singapore under grant M4061216.057, by NTU under grant M4080181.050 and by MOE AcRF grant RG 33/10 M4010492.050.

indistinguishable as a network degenerates. A more detailed discussion of 12 important robustness measures can be further found in [14].

The algebraic connectivity can be a fair measure to evaluate the structural robustness of the air transportation network as shown in [15], [16], *i.e.*, the larger the algebraic connectivity is, the more difficult the network can be separated when facing random link failures. Although the algebraic connectivity is a good measure for the global connectivity of the entire network, it may fail to capture the change of the local network characteristics after edge addition/deletion or edge weight perturbation.

In this paper, we propose to measure the robustness of air transportation network by the total effective resistance. The effective resistance between a pair of nodes i and j, denoted $R_{i,j}$, is the electrical resistance measured across these two nodes when the network represents an electrical circuit with each edge regarded as a resistor with an electrical conductance of $w_{i,j}$. In other words, $R_{i,j}$ is the potential difference that appears across terminals i and j when a unit current source is applied between them. $R_{i,j}$ is relatively smaller when the nodes i and j are connected with more paths associated with higher conductance edges. The total effective resistance R_{tot} is the sum of $R_{i,j}$ between all distinct pairs of nodes (i, j), which can be reduced by adding more edges or increasing edge conductance. More interpretations of effective resistance are available in [17]. It has been shown in [18], [19] that the total effective resistance can quantify a number of important properties and performance metrics of a network, such as coherence, consensus rate, and robustness. The air transportation network is an analogy to the electrical circuit network, where a route with a failure rate of $1/w_{i,j}$ can be regarded as a resistor with a conductance of $w_{i,j}$. Smaller $R_{i,j}$ means that nodes i and j are connected with more paths associated with routes with lower failure rates, which implies the network robustness for linking i and j. Since $R_{\text{tot}} = \sum_{i<j} R_{i,j}$, it can be used to measure the robustness of the entire network. Moreover, the total effective resistance can not only capture the global property of the average or aggregate network characteristics but also distinguish the changes of an individual node or edge, as demonstrated in Section II below.

A. Related Work

The following two areas of studies are highly related to this work: 1) structural robustness analysis and optimization of air transportation networks, and 2) evaluation and optimization of various types of networks using total effective resistance.

Since the small-world phenomenon [20] and the scale-free characteristic [21] were discovered, an increasing number of researchers explored the applications of network theory into air transportation networks. Guimera and Amaral first presented an exhaustive analysis of the worldwide airport network; they discovered that the network is a small-world network with a power-law decaying degree and betweenness distribution [1]; similar claims on the worldwide airport network were made in [22]. Bonnefoy found that the air transportation network is not scale-free and scalable due to capacity constraints at major airports; however, the network become scale-free when multiple airports are aggregated into single nodes [23]. He also used the degree distribution of the existing light jet network to understand the potential impacts of very light jets [24]. DeLaurentis *et al* selected several statistical measures to analyze the connectivity in air transportation networks and then derived implications from both local and global topology characteristics [10]. Kotegawa *et al* utilized different nodal metrics including node degree, eigenvector centrality, and clustering coefficient as predictor variables and then estimated the airport topology by their machine learning method [25]. Azzam *et al* used degree distribution to study the worldwide air transportation network and showed that it is non-stationary and subject to densification and accelerated growth [26]. Sun *et al* studied the temporal evolution of seven centrality measures for air navigation route networks and airport networks, which were beneficial to better understand the network dynamics [27]. They also used the similarity scores computed by functionally independent metrics to assess the structural similarity of air navigation route networks [28]. A small group of researchers has explored the structural optimization of air transportation networks. Reggiani *et al* analyzed the connectivity and concentration of Lufthansa's network and then proposed a multi-criteria analysis to strategically configure the airline network patterns [29]. Wullner *et al* introduced two network rewiring schemes, called "Diamond" and "Chain", that can boost resilience to different levels of perturbation while preserving a total number of flight and gate requirements [30]. Cai *et al* investigated the application of computational intelligence to crossing waypoints location problem in the context of real-world air route network design [31]. In [32], Hong *et al* investigated the structural properties of the Chinese air transportation multilayer network by using global network efficiency, connectivity, assortativity, etc. Linkov *et al* provided a synopsis for understanding current shortcomings of quantitative methods for addressing the complexities of large integrated networks in [9]. Moreover, there are a body of works focusing on using percolation approaches to study the tolerance to errors and attacks in air transportation networks [33], [34]. In [35], Schneider *et al* introduced a new robustness measure based on the size of the largest component and used it to devise an efficient and economical method to mitigate the network risk and improve the robustness of existing infrastrcutures. In [36], Latora *et al* introduced the measure of network efficiency, an alternative to the average path length, to perform a precise quantitative analysis for both weighted and unweighted networks. It should be noted that although network efficiency can be measured with a high computational efficiency, since network efficiency is defined based on the shortest path between node pairs, it doesn't incorporate the characteristics of alternative paths that may also be important for evaluating network robustness.

The most relevant and closely related measure is the algebraic connectivity, which has been intensively investigated in air transportation community. Vargo *et al* explored the effectiveness of a tabu search algorithm and semidefinite programming relaxation to increase the algebraic connectivity of air transportation networks [37]. Wei *et al* proposed three approaches to maximize the algebraic connectivity of air transportation networks in [15]. Furthermore, they formulated a new air transportation network optimization problem considering both edge addition and weight assignment and solved the algebraic connectivity optimization problem for different network scales [16].

There is a handful of literature on the application of effective resistance in various types of networks. Ghosh *et al* studied the problem of allocating edge weights on a given weighted network to minimize the total effective resistance [17]. Van Mieghem *et al* showed the qualitative relationship between effective resistance and graph associativity, a correlation of the similarities of nodes sharing a link [38]. Wang *et al* derived the upper and lower bound of the total effective resistance under scenarios of edge addition and deletion, then they introduced four strategies for adding/deleting an edge that minimizes/maximizes the total effective resistance [19]. Ellens *et al* concerned the optimal addition of one edge for graphs with given number of vertices and diameter to minimize the total effective resistance [39].

In this paper, we measure and optimize the robustness of air transportation networks by the total effective resistance. The strategies to enhance the network can be divided into four categories, *i.e.*, edge rewiring [40], [41], edge addition [15], [42], weights assignment [17], and the combination of edge addition and weight assignment [16]. In this study, we consider the edge addition strategy, in which a few routes are selected to be added into the existing air transportation network. Compared to the edge rewiring strategy that fixes the total number of edges, the edge addition strategy allows k extra edges to be added into the existing network when airlines have a budget and are particularly interested in expanding their networks.

B. Contribution

The main contributions of this work are summarized as follows:

1) a comparative study is conducted to show that the total effective resistance is a more promising robustness measure than the algebraic connectivity;
2) this work for the first time adopts the total effective resistance to measure and optimize the robustness of air transportation networks;
3) to solve the corresponding flight route selection problem, a difficult integer nonlinear programming problem, we develop two methods for different network scales to balance the trade-off between computation time and optimality performance in terms of the total effective resistance. An interior-point method based on convex relaxation and duality gap is developed for small/medium-scale networks, which achieves a near optimality performance within acceptable time. An accelerated greedy algorithm based on proved monotone submodularity is developed for large-scale networks, which can substantially reduce the computation time in deriving a good solution with a guaranteed optimality gap;
4) three case studies from real world examples are performed to demonstrate the application of the proposed methods.

The rest of this paper is organized as follows. In Section II, two comparative studies of robustness measures are conducted. In Section III, the flight route selection problem is formulated based on the total effective resistance. In Sections IV and V, two efficient methods are developed for different scale networks respectively. In Section VI, numerical experiments and three case studies are performed to verify the performance of the two methods. Section VII concludes this paper.

II. Comparison of Robustness Measures

As mentioned before, since the algebraic connectivity is the most close and relevant robustness measure to the total effective resistance adopted in this paper, we mainly compare these two measures in this section. A more comprehensive comparative study for 12 robustness measures we recently conducted can be found in [14].

Before proceeding to the comparison, we will first demonstrate that these two measures can essentially capture network structural robustness in the following subsection.

A. Network Structural Robustness

Like the total effective resistance (denoted by R_{tot}), the algebraic connectivity (denoted by λ_2) can also be fair to measure how well a network is connected [16]. The algebraic connectivity λ_2, the second smallest eigenvalue of Laplacian matrix, can determine the connectivity of a graph (network) G by checking whether $\lambda_2 > 0$.

Since the two measures R_{tot} and λ_2 are still quite abstract, we will introduce a straightforward and intuitive metric that can capture network structural robustness and use it as a reference to show both of them can also essentially measure structural robustness.

The total number of acyclic paths between all node pairs (denoted by Q) can be a good candidate to serve as the reference. Clearly, the higher Q, the more alternative routes between nodes, which implies a more robust network structure.

In the following, we will conduct Monte Carlo simulation experiments on 500 randomly generated networks with 8 nodes and 17 edges. For each randomly generated network, k edges will be gradually and randomly removed one by one until $k = 7$. The statistical results are recorded in Table I. It can be observed that as more edges are removed from networks, Q monotonically decreases while R_{tot} monotonically increases and λ_2 monotonically decreases, which demonstrates the strong correlation between $R_{\mathrm{tot}}, \lambda_2$ and Q. In other words, the less the total number of acyclic paths between all node pairs, the higher the total effective resistance and the lower the algebraic connectivity. Therefore, the structural robustness can be optimized by either maximizing Q or minimizing R_{tot} or maximizing λ_2.

TABLE I
THE MONTE CARLO SIMULATION RESULTS OF Q, R_{tot}, AND λ

Removal edges	Q (mean, var)	R_{tot}(mean, var)	λ (mean, var)
$k=1$	(2849.49, 111.66)	(15.65, 0.28)	(2.00, 0.07)
$k=2$	(2027.81, 314.04)	(17.42, 1.28)	(1.80, 0.11)
$k=3$	(1511.41, 356.22)	(19.21, 1.86)	(1.61, 0.31)
$k=4$	(1170.63, 325.90)	(21.12, 2.46)	(1.50, 0.28)
$k=5$	(941.85, 334.47)	(23.01, 2.93)	(1.20, 0.37)
$k=6$	(799.27, 278.04)	(24.46, 3.28)	(1.05, 0.35)
$k=7$	(712.53, 269.55)	(25.71, 3.69)	(1.01, 0.39)

It should be noted that adopting Q as an objective function is inefficient for optimizing structural robustness because Q cannot be expressed in a closed form and computing Q generally requires an exponential time complexity. In contrast, R_{tot} can be evaluated in $O(n^3)$ and is more suitable for the optimization considered in this paper.

B. Total Effective Resistance vs Algebraic Connectivity

Although the algebraic connectivity λ_2 is shown to be a fair measure of air transportation network [16], it is still a measure for the global connectivity of the entire network and may not be able to capture the local characteristics.

The total effective resistance R_{tot} can be connected to the algebraic connectivity by the bounds shown in [39], $\frac{n}{\lambda_2} < R_{\text{tot}} \leq \frac{n(n-1)}{\lambda_2}$, which implies the possibility of using the total effective resistance to substitute the algebraic connectivity. Moreover, the total effective resistance is capable of reflecting both the global and local characteristics in measuring the network robustness. We conduct the comparative experiment on the air transportation network of Tigerair Australia in Fig. 1, consisting of 14 airports (squares) and 21 routes (red lines).

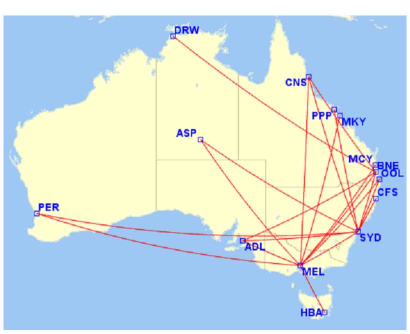

Fig. 1. Air transportation network of Tigerair Australia in 2015

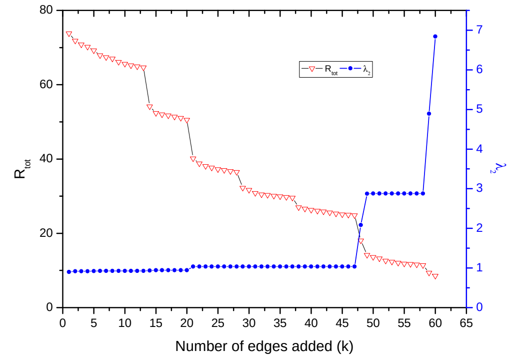

Fig. 2. R_{tot}, λ_2 in terms of random route addition for Tigerair Australia

The weights of all the edges in the network in Fig. 1 are uniformly sampled from the following three values, $w_{i,j} = \{1, 2, 3\}$, which represent the link strengths. A larger weight indicates that the route is more robust to disruptions. In each iteration of the experiment, one candidate edge is randomly selected and added it into the existing network. The comparison results are depicted in Fig. 2. It can be observed that both the total effective resistance and the algebraic connectivity are monotonic with the addition of edges. This similarity indicates that the total effective resistance can be used to reflect the robustness of network like the algebraic connectivity. Moreover, the total effective resistance can always distinguish the gradual change when an edge is added. When increasing k from 21 to 45, the total effective resistance gradually decreases, whereas the algebraic connectivity remains unchanged.

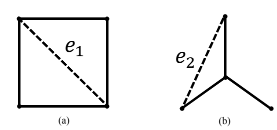

Fig. 3. Two small scale networks with four nodes

The two small scale networks in Fig. 3 can be more insightful to interpret this effect. Let ΔR_{tot} and $\Delta\lambda_2$ denote the changes of total effective resistance and algebraic connectivity respectively after adding an edge. For the example in Fig. 3(a), when the edge e_1 with $w_1 = 1$ is added, $\Delta R_{\text{tot}}/R_{\text{tot}} = 0.2$ and $\Delta\lambda_2/\lambda_2 = 0$. For the example in Fig. 3(b), when the edge e_2 with $w_2 = 3$ is added, $\Delta R_{\text{tot}}/R_{\text{tot}} = 0.3$ and $\Delta\lambda_2/\lambda_2 = 0$. Moreover, even when the edge weights are assigned as $+\infty$ for both e_1 and e_2, $\Delta\lambda_2$ still remains zero. Nonetheless, the network robustness has been actually improved after adding e_1 and e_2 because air traffic can be more flexibly transferred via the added edges. Therefore, since the total effective resistance can capture the global and local characteristics of air transportation networks, it is more promising to measure and optimize the network robustness.

III. PROBLEM FORMULATION

A. Total Effective Resistance

The total effective resistance is adopted to measure the robustness of an air transportation network, which is generally composed of a set of airports and flight routes connecting them. Since the vast majority of flight routes between airports are two-way routes as mentioned in the introduction, we model an air transportation network as an undirected and connected graph $G = (V, E)$, where $|V| = n$ and $|E| = m$. Suppose edge e connects node i and j, we define $h_e \in \mathbf{R}^n$ as $(h_e)_i = 1$, $(h_e)_j = -1$, and all the other entries are 0. Let $A \in \mathbf{R}^{n\times m}$ denote the incidence matrix of the graph G, *i.e.*, $A = [h_1, h_2..., h_m]$. Then the Laplacian matrix L of the weighted graph G can be expressed as $L = \sum_{e=1}^{m} w_e h_e h_e^T = A\mathbf{Diag}(W)A^T$, where W is the nonnegative weight vector whose components are associated with corresponding edges and $\mathbf{Diag}(W) \in \mathbf{R}^{m\times m}$ is the diagonal matrix constructed from W.

The total effective resistance R_{tot} is defined as the following summation, $R_{\text{tot}} = \sum_{i<j} R_{i,j}$, where $R_{i,j}$ is the effective resistance between a pair of nodes i and j. Since $R_{i,j} = R_{j,i}$, the summation only applies to the node pairs with $i < j$. Furthermore, as shown in [17], the total effective resistance can be expressed as

$$R_{\text{tot}} = n\mathbf{tr}(L + \mathbf{1}\mathbf{1}^T/n)^{-1} - n \tag{1}$$

where $\mathbf{tr}(\cdot)$ is the trace of a square matrix and $\mathbf{1}$ is the vector with all entries one.

B. Flight Route Selection Problem

Now we can describe the flight route selection problem. Since many airlines have already set up certain air transportation networks to provide services in local or worldwide regions, it is not necessary to create an entirely new air transportation network from scratch. Most likely in practice, we will face a flight route selection problem, in which a few extra routes are selected from a set of potentially available and viable routes and added into the existing network to improve the robustness. We would like to develop an optimal and efficient way in selecting edges.

Let (V, E_0) represent the existing air transportation network with the initial edge set E_0 consisting of the existing routes between the airports in V and let E_P denote the set of extra edges for improving robustness. The objective is to minimize the total effective resistance R_{tot} of the new network with k edges selected from the given edge set E_P and added into the existing network (V, E_0). Assume $|E_P| = p \geq k$ and $E_P = \{1, ..., p\}$. From (1), the total effective resistance R_{tot} can be effectively computed through the weighted Laplacian matrix. Then the corresponding augmented Laplacian matrix of the new network can be expressed as follows, $L = L_0 + \sum\limits_{e=1}^{p} y_e w_e h_e h_e^T$, where L_0 is the Laplacian matrix of the existing network and y_e is a Boolean variable to indicate whether the edge e is selected from E_P. Finally, the flight route selection problem can be formulated as,

$$\begin{array}{ll} \underset{y_1,\dots,y_p}{\text{minimize}} & R_{\text{tot}}(L_0 + \sum_{e=1}^{p} y_e w_e h_e h_e^T) \\ \text{subject to} & \mathbf{1}^T y = k, \\ & y_e \in \{0,1\}, \quad e = 1, ..., p. \end{array} \tag{2}$$

where $y = [y_1, ..., y_p]^T$ and $R_{\text{tot}}(\cdot)$ is a function of a Laplacian matrix. The problem (2) is a Boolean-convex problem [43] because the objective function is convex in $0 \leq y \leq 1$ as shown in Theorem 1 in Section IV-A and the constraint is linear.

IV. Convex Relaxation

The flight route selection problem in (2) is an integer nonlinear programming problem. Clearly, a brute force method of enumerating all $\binom{p}{k}$ route combinations is not practical in solving the problem unless k and p are small. In this section, we will develop an interior-point algorithm based on the analysis of the duality gap of its convex relaxation.

A. Convex Relaxation of Flight Route Selection Problem

The original flight route selection problem (2) can be relaxed by replacing the original binary variables with the continuous variables $y_e \in [0, 1]$ for $e = 1, ..., p$ as follows,

$$\begin{array}{ll} \underset{y_1,\dots,y_p}{\text{minimize}} & n\mathbf{tr}(L_0 + \sum_{e=1}^{p} y_e w_e h_e h_e^T + \mathbf{1}\mathbf{1}^T/n)^{-1} - n \\ \text{subject to} & \mathbf{1}^T y = k, \\ & 0 \leq y_e \leq 1, \quad e = 1, ..., p \end{array} \tag{3}$$

This relaxed flight route selection problem (3) can be proved to be convex through the following theorem. (For the continuity of reading, all the proofs are placed in the Appendix in this paper.)

Theorem 1. *The total effective resistance function $R_{\text{tot}}(y) = n\mathbf{tr}(L(y) + \mathbf{1}\mathbf{1}^T/n)^{-1} - n$ is convex in y, where $L(y) = L_0 + \sum_e y_e w_e h_e h_e^T$.*

Based on Theorem 1, the objective function of the relaxed problem (3) is convex. Combining it with the fact of the linear constraints, we can show that the relaxed problem (3) is a convex programming problem. The problem (3) can be further equivalently converted to a semidefinite programming problem (SDP) of minimizing a linear objective function, whose feasible solutions are symmetric positive semidefinite matrices, subject to additional linear constraints. Although it provides an opportunity to solve the problem (3) using a well-developed SDP solver such as SeDuMi [44], we can develop an interior-point algorithm based on the duality gap of the problem (3), which is much more efficient than solving it as an SDP problem.

B. Dual Problem of Relaxed Flight Route Selection Problem

In this section, we formulate the dual problem of the relaxed flight route addition problem for deriving the duality gap.

Firstly, we introduce a new variable $X = L_0 + \mathbf{1}\mathbf{1}^T/n + \sum_{e=1}^{p} y_e w_e h_e h_e^T$ and reformulate the problem (3) as the following problem with the variables $y \in \mathbf{R}^p$ and $X \in \mathbf{S}^n$ (the set of symmetric $n \times n$ matrices):

$$\begin{array}{ll} \underset{y}{\text{minimize}} & n\mathbf{tr}X^{-1} - n \\ \text{subject to} & X = L_0 + \sum_{e=1}^{p} y_e w_e h_e h_e^T + \mathbf{1}\mathbf{1}^T/n, \\ & \mathbf{1}^T y = k, \\ & 0 \leq y \leq 1. \end{array} \tag{4}$$

Secondly, we introduce the Lagrange multipliers λ for $y \geq 0$, μ for $y \leq 1$, ν for $\mathbf{1}^T y = k$, and Λ for $X = L_0 + \sum_{e=1}^{p} y_e w_e h_e h_e^T + \mathbf{1}\mathbf{1}^T/n$ to form the Lagrangian of the problem (4) as follows:

$$
\begin{aligned}
&\mathrm{L}(y, X, \Lambda, \lambda, \mu, \nu) \\
&= \mathbf{tr}(\Lambda(X - L_0 - \sum\nolimits_{e=1}^{p} y_e w_e h_e h_e^T - \mathbf{1}\mathbf{1}^T/n)) \\
&\quad + n\mathbf{tr}X^{-1} - \lambda^T y + \mu^T(\mathbf{1}^T y - k) + \nu^T(y-1) - n. \\
&= (\sum\nolimits_{e=1}^{p} y_e(-w_e h_e \Lambda h_e^T - \lambda_e + \mu_e + \nu_e)) - (1/n)\mathbf{1}\Lambda\mathbf{1}^T \\
&\quad + \mathbf{tr}(nX^{-1} + X\Lambda) - \mathbf{tr}(\Lambda L_0) - \mathbf{1}^T\mu - \nu k - n.
\end{aligned}
$$

where $\lambda \in \mathbf{R}^p$, $\mu \in \mathbf{R}^p$ are non-negative, $\nu \in \mathbf{R}$, and $\Lambda \in \mathbf{S}^n$.

The Lagrange dual function g is given by

$$g(\Lambda, \lambda, \mu, \nu) = \inf_{y,X} \mathrm{L}(y, X, \Lambda, \lambda, \mu, \nu).$$

Since the minimization of L is bounded only if

$$\lambda_e - \mu_e - \nu_e + w_e h_e \Lambda h_e^T = 0,$$

the Lagrange dual function g holds that

$$
g(\Lambda, \lambda, \mu, \nu) = \begin{cases} 2\mathbf{tr}(n\Lambda)^{1/2} - (1/n)\mathbf{1}\Lambda\mathbf{1}^T - \mathbf{tr}(\Lambda L_0) \\ -\mathbf{1}^T\mu - \nu k - n, \\ \qquad\qquad \text{if} \;\; \lambda_e - \mu_e = \nu_e - w_e h_e \Lambda h_e^T, \\ \infty, \qquad\qquad\qquad\qquad \text{otherwise.} \end{cases}
$$

To justify the equality, we note that $\mathbf{tr}(nX^{-1} + X\Lambda)$ is unbounded below, as a function of X, unless $\Lambda \succeq 0$; when $\Lambda \succ 0$, the unique X that minimizes it is $X = (\Lambda/n)^{-1/2}$ and the corresponding minimal value is

$$
\begin{aligned}
\mathbf{tr}(nX^{-1} + X\Lambda) &= \mathbf{tr}\left(n(\Lambda/n)^{1/2} + \Lambda(\Lambda/n)^{-1/2}\right) \\
&= 2\mathbf{tr}(n\Lambda)^{1/2}.
\end{aligned}
$$

Finally, the dual problem of the relaxed flight route selection problem can be formulated as

$$
\begin{aligned}
\text{maximize} \quad & 2\mathbf{tr}(n\Lambda)^{1/2} - (1/n)\mathbf{1}\Lambda\mathbf{1}^T - \mathbf{tr}\Lambda L_0 - \mathbf{1}^T\mu \\
& - \nu k - n \\
\text{subject to} \quad & \lambda_e = \mu_e + \nu - w_e h_e \Lambda h_e^T, \quad e = 1, ..., p, \\
& \lambda_e \geq 0, \; \mu_e \geq 0, \quad e = 1, ..., p.
\end{aligned} \tag{5}
$$

After eliminating the variables λ_e, it can be further equivalently reduced to the problem (6) below,

$$
\begin{aligned}
\underset{\mu, v}{\text{maximize}} \quad & 2\mathbf{tr}(n\Lambda)^{1/2} - (1/n)\mathbf{1}\Lambda\mathbf{1}^T - \mathbf{tr}(L_0\Lambda) \\
& - \mathbf{1}^T\mu - k\nu - n \\
\text{subject to} \quad & w_e h_e^T \Lambda h_e \leq v + \mu_e, \quad e = 1, ..., p, \\
& \mu_e \geq 0, \quad e = 1, ..., p.
\end{aligned} \tag{6}
$$

where $\Lambda \in \mathbf{S}^n$, $\mu \in \mathbf{R}^p$, and $\nu \in \mathbf{R}$.

C. Duality Gap

The dual problem (6) itself is a convex programming problem with $\Lambda \in \mathbf{S}^n$, $\mu \in \mathbf{R}^p$, and $\nu \in \mathbf{R}$. The Lagrange multipliers can be eliminated because the optimal value is obviously $\mu_e + \nu = \max_e(w_e h_e^T \Lambda h_e)$. Since the dual problem (6) is a maximization problem, we have $\mu = 0$ and $\nu = \max_e(w_e h_e^T \Lambda h_e)$. Since the primal problem (4) has only linear equality and inequality constraints, the convex Slater's condition can be satisfied when $y = (k/p)\mathbf{1}$. Hence the optimal gap between the primal and dual problem is zero. If X^* is the optimal solution of the primal problem (4), then $\Lambda^* = n(X^*)^{-2}$, $\nu^* = \max_e(w_e h_e^T \Lambda^* h_e)$, $\mu = 0$ are the optimal solution of the dual problem (6). Conversely, if Λ^* is the optimal solution of the dual problem, then $X^* = (\Lambda^*/n)^{-1/2}$ is the optimal solution of the primal problem (4).

From the analysis above, a duality gap δ can be derived by Theorem 2 below, which is useful to measure the suboptimality of any feasible solution y. An interior-point algorithm can be accordingly developed based on the duality gap δ.

Theorem 2. *Let $L = L_0 + \sum_{e=1}^{p} y_e w_e h_e h_e^T$ and $S = (\Lambda, \mu, \nu)$ denote a feasible solution of the dual problem (6), where $\Lambda = n(L + \mathbf{1}\mathbf{1}^T/n)^{-2}$, $\nu = \max_e(w_e h_e^T \Lambda h_e)$ and $\mu = 0$. And y is the edge vector associated with S. Then the duality gap δ with respect to S is*

$$\delta = -\max_e(R_{\text{tot}} + k w_e^{-1}\frac{\partial R_{\text{tot}}}{\partial y_e} - n\mathbf{tr}(L_0(L + \mathbf{1}\mathbf{1}^T/n)^{-2})).$$

D. Interior-Point Algorithm

In this section, we develop an interior-point algorithm, namely, a barrier method, with the help of the duality gap δ in Theorem 2 to efficiently solve the relaxed flight route selection problem (3).

We adopt logarithmic barrier functions to implicitly include the inequality constraints in the problem (3) in the objective function and approximately formulate the problem (3) as follows:

$$
\begin{aligned}
\underset{y}{\text{minimize}} \quad & \psi(y) = R_{\text{tot}}(y) - \gamma \sum_{e=1}^{p} \big(\log(y_e) + \log(1 - y_e)\big) \\
\text{subject to} \quad & \mathbf{1}^T y = k
\end{aligned} \tag{7}
$$

where γ is a small positive scalar and called the barrier parameter that controls the quality of approximation. Let $\tilde{y}$ and y^* denote the optimal solution of the problem (7) and (3) respectively. As shown in the Section 11.2 of [45], $\tilde{y}$ is at most $2p\gamma$ suboptimal for the relaxed flight route selection problem (4), that is,

$$R_{\text{tot}}(\tilde{y}) - R_{\text{tot}}(y^*) \leqslant 2p\gamma. \tag{8}$$

It provides an opportunity to achieve y^* by solving a sequence of decreasing values of γ until $\gamma \leq \epsilon/2p$ which guarantees an ϵ-optimal solution of the original problem (3). In the barrier method, we can use the duality gap δ to construct the sequence of decreasing values of γ by setting $\gamma = \beta\delta/2p$, where β is some constant within $(0, 1]$. Combining it with (8), it holds that

$$R_{\text{tot}}(\tilde{y}) - R_{\text{tot}}(y^*) \leqslant 2p * \beta\delta/2p \leqslant \delta. \tag{9}$$

We start with the initial solution as $y = (k/p)\mathbf{1}$. In each iteration, we apply the Newtons' method to compute the search direction Δy_{nt} as

$$\Delta y_{nt} = -(\nabla^2\psi)^{-1}\nabla\psi + \left(\frac{\mathbf{1}^T(\nabla^2\psi)^{-1}\nabla\psi}{\mathbf{1}^T(\nabla^2\psi)^{-1}\mathbf{1}}\right)(\nabla^2\psi)^{-1}\mathbf{1}.$$

in which the gradient of ψ is

$$(\nabla\psi)_e = -n\mathbf{tr}(\bar{L}_E(y))^{-1}h_{e,w}h_{e,w}^T\mathbf{tr}(\bar{L}_E(y))^{-1} + \frac{\gamma}{y_e} - \frac{\gamma}{(1 - y_e)}$$

for $e = 1, ..., p$ and the Hessian of ψ is

$$\nabla^2\psi = 2n(A_w^T(\bar{L}_E(y))^{-2}A_w) \circ (A_w^T(\bar{L}_E(y))^{-1}A_w) \\ - \gamma \text{diag}\left(\frac{1}{y_1^2} + \frac{1}{(1-y_1)^2}, ..., \frac{1}{y_p^2} + \frac{1}{(1-y_p)^2}\right)$$

where $\circ$ denotes the Hadamard product, $h_{e,w} = w_e^{\frac{1}{2}} h_e$, $A_w = [h_{1,w} \cdots h_{p,w}]$, and $\bar{L}_E(y) = L_0 + \sum_e y_e w_e h_e h_e^T + \mathbf{1}\mathbf{1}^T/n$. We then compute the step size $s \in (0, 1]$, and update y as $y + s\Delta y_{nt}$. The search process will be terminated when the duality gap δ is reduced to an acceptable value.

Algorithm 1 Interior-Point Algorithm

Input: relative tolerance $\varphi \in (0, 1)$, $0 < \beta < 1$.
Initialize $\tilde{y} \leftarrow (k/p)\mathbf{1}$.
while $\delta > \varphi R_{\text{tot}}(y)$ **do**
  Set $\gamma \leftarrow \beta\delta/p$.
  Compute Newton step $\delta\tilde{y}_{nt}$ for $\psi(\tilde{y})$ by solving
  $\Delta\tilde{y}_{nt} = -(\nabla^2\psi)^{-1}\nabla\psi + (\frac{\mathbf{1}^T(\nabla^2\psi)^{-1}\nabla\psi}{\mathbf{1}^T(\nabla^2\psi)^{-1}\mathbf{1}})(\nabla^2\psi)^{-1}\mathbf{1}$.
  Find the step length s by backtracking line search.
  $\tilde{y} \leftarrow \tilde{y} + s\Delta\tilde{y}_{nt}$.
end while
return R_{tot}, $\tilde{y}$.

The interior-point algorithm is summarized in Algorithm 1. The final solution $\tilde{y}$ obtained by Algorithm 1 satisfies the termination condition $\delta \leqslant \varphi R_{\text{tot}}(\tilde{y})$ and the condition in (9) ensuring that $R_{\text{tot}}(\tilde{y}) - R_{\text{tot}}(y^*) \leqslant \delta$, which implies $\frac{R_{\text{tot}}(\tilde{y}) - R_{\text{tot}}(y^*)}{R_{\text{tot}}(y^*)} \leqslant \frac{\varphi}{1-\varphi}$. Thus, Algorithm 1 can guarantee to derive an edge vector for the relaxed flight route selection problem (3) with a relative optimality gap less than $\varphi/(1-\varphi)$.

Since the solutions of the relaxed problem $\tilde{y}$ obtained by Algorithm 1 are not necessarily 0-1 integers, step by step rounding methods can be employed here to construct a good approximation of the optimum from $\tilde{y}$. All the steps are summed up in Algorithm 2. In each iteration, we select the maximal element from $\tilde{y}$ and update the Laplacian by adding this edge in the approximate flight route selection problem. Then we resolve this problem and iterate till k edges are added.

Algorithm 2 Interior-point algorithm with step by step rounding technique

Input: weighted graph $G(V, E_0)$, w_e for each $e \in E_P$.
Solve problem (7) with k.
for $i = 1$ to k **do**
  $j \leftarrow \arg\max_e\{y_e | y_e \leq 1\}$.
  $\hat{y}_j \leftarrow 1$.
  Solve problem (7) with $k - i$ (**Algorithm 1**).
end for
return R_{tot}, $\hat{y}$

V. SUBMODULAR GREEDY ALGORITHM

The convex relaxation method developed above is still subject to the curse of dimensionality, albeit having a near optimality performance and an acceptable computational efficiency for small/medium-scale networks. The most time-consuming step in Algorithm 2 is solving the problem (7), whose computation time exponentially increases with the growth of the number of nodes n as shown in the numerical results below. To approach a large-scale problem that contains more than hundred nodes, we will further develop a submodular greedy algorithm which provides a promising optimality performance within practical time limits.

A. Submodularity of R_{tot}

The flight route selection problem (2) can be regarded as a set function problem (10) below if let $f(S) = -R_{\text{tot}}(S)$.

$$\begin{aligned} \underset{S \subseteq E}{\text{maximize}} \quad & f(S) \\ \text{subject to} \quad & |S| = k \end{aligned} \tag{10}$$

where $f : 2^E \rightarrow \mathbf{R}$ is a set function that assigns a real number to each subset of E. It can be proved that the set function $f(S) = -R_{\text{tot}}(S)$ is monotone submodular as shown in Theorem 3 below.

Theorem 3. *Given a graph $G(V, E_0)$. The set function $f(E) = -R_{tot}(E_0 \cup E)$ is monotone submodular for $E \subseteq E_P$, that is, for any $A \subseteq B \subseteq E_P$ and $e \in E_P \backslash B$, $f(A) \leq f(B)$ and $f(A \cup \{e\}) - f(A) \geq f(B \cup \{e\}) - f(B)$.*

The submodularity is such a promising property of the set functions with solid theoretical background [46] and far-reaching applications [47], [48], [49]. In combinatorial optimization, submodularity is the counterpart of convexity (concavity) in continuous optimization.

The submodularity exhibits a natural characteristic of diminishing gains, *i.e.*, adding an element e to a larger set gives a smaller marginal benefit than adding one to a smaller subset. It enables a greedy algorithm to efficiently obtain a good solution with a guaranteed optimality gap as shown in Theorem 4 below.

Theorem 4. *Let $R_{\text{tot}}^{\text{OPT}}$ denote the function value of an optimal solution to problem (2) and $R_{\text{tot}}^{\text{G}}$ denote the one of the solution derived by the greedy algorithm (Algorithm 3 below). Then it holds that*

$$R_{\text{tot}}^{\text{G}} \leq (1 + \frac{\alpha - 1}{e})R_{\text{tot}}^{\text{OPT}}$$

where $\alpha = \frac{R_{\text{tot}}(E_0)}{R_{\text{tot}}^*}$ and R_{tot}^* is the minimal function value achieved by adding all the candidate edges.

B. Submodular Greedy Algorithm

As shown in Theorem 4, the greedy algorithm (Algorithm 3) can efficiently obtain a solution with a guaranteed optimality gap, in which Line 1 initializes a solution, Line 3 selects the edge from E_P which makes the maximal decrease in terms of R_{tot}, and Line 4 makes addition and deletion operations on E_S and E_P respectively.

Algorithm 3 is only a basic greedy algorithm and it can be still computationally intensive if the marginal function in Line 3 cannot be efficiently evaluated and optimized, especially when facing a large-scale network with a huge $|E_p|$. With the help of Theorem 5 below, instead of separately computing R_{tot} for two different networks, the marginal function in Line 3 of Algorithm 3 can be more efficiently evaluated by (11), which paves the way for the accelerated submodular greedy algorithm in Algorithm 4.

Algorithm 3 Basic submodular greedy algorithm

Input: weighted graph $G(V, E_0)$, w_e for $e \in E_P$.
Initialize $E_S \leftarrow E_0$.
while $|S| \leq k$ **do**
  $e \leftarrow \arg\max_{e \in E_P} [R_{\text{tot}}(E_S) - R_{\text{tot}}(E_S \cup e)]$.
  $E_S \leftarrow E_S \cup e$, $E_P \leftarrow E_P \backslash e$.
end while
return R_{tot}, S.

Theorem 5. *Given any connected weighted network $G(V, E)$ with weighted Laplacian matrix L_E, any edge $e \in E_P$ for addition with weight w_e, and incidence matrix h_e, then*

$$R_{\text{tot}}(E) - R_{\text{tot}}(E \cup e) = \frac{n w_e}{\beta} \|(L_E + 11^T/n)^{-1} h_e\|^2 \qquad (11)$$

where $\beta = 1 + w_e h_e^T (L_E + \mathbf{11}^T/n)^{-1} h_e$.

Although (11) in Theorem 5 simplifies the evaluation of the marginal function, it may still suffer from the computational burden resulted from computing $(L_{E_S} + \mathbf{11}^T/n)^{-1}$. Fortunately, since only one edge e will be added into E_s every iteration, after calculating $(L_{E_0} + \mathbf{11}^T/n)^{-1}$ in the first iteration, $(L_{E_S} + \mathbf{11}^T/n)^{-1}$ can be efficiently derived by performing a rank-1 update in the following iterations, which finally enables the accelerated submodular greedy algorithm developed in Algorithm 4. In Line 2, the inverse of $L_{E_0} + \mathbf{11}^T/n$ can be efficiently obtained by the conjugate gradient method [50] in the complexity of $\mathcal{O}(\kappa\sqrt{\upsilon})$, where κ is the number of nonzero entries in $(L_{E_0} + \mathbf{11}^T/n)$ and υ is its condition number. Line 4 uses (11) to evaluate each edge in E_P and chooses the one with the largest marginal decrease, in which $(L_{E_S} + \mathbf{11}^T/n)^{-1}$ is commonly computed using the Sherman-Morrison formula [51], [52], [53] to perform the rank-1 updates to the inverse matrix derived in the previous iteration in the complexity of $\mathcal{O}(n^2)$. Line 5 and 6 just update $R_{\text{tot}}(E_S)$, E_S and E_P. The total computational complexity of the accelerated submodular greedy algorithm is about $\mathcal{O}(\kappa\sqrt{\upsilon} + kn^2)$.

Algorithm 4 Accelerated submodular greedy algorithm

Input: weighted graph $G(V, E_0)$, w_e for $e \in E_P$.
1: Initialize $E_S \leftarrow E_0$.
2: Compute $(L_{E_S} + \mathbf{11}^T/n)^{-1}$ with the conjugate gradient method and then let $R_{\text{tot}}(E_S) \leftarrow n\mathbf{tr}(L_{E_S} + \mathbf{11}^T/n)^{-1} - n$.
3: **while** $|S| \leq k$ **do**
4:   $e \leftarrow \arg\max_{e \in E_P} \frac{n w_e}{\beta} \|(L_{E_S} + 11^T/n)^{-1} h_e\|^2$.
5:   $R_{\text{tot}}(E_S) \leftarrow R_{\text{tot}}(E_S) - \frac{n w_e}{\beta} \|(L_{E_S} + 11^T/n)^{-1} h_e\|^2$.
6:   $E_S \leftarrow E_S \cup e$, $E_p \leftarrow E_p \backslash e$.
7: **end while**
8: **return** R_{tot}, S .

VI. Numerical Results & Case Studies

A. Convex Relaxation vs. Submodular Greedy Algorithm

We compare the performance of the submodular greedy algorithm and the convex relaxation method with step by step rounding technique. Both of them are programmed using MATLAB R2016a on a desktop computer with 2.70GHz Intel(R) Core(TM) i7 CPU and 8GB RAM in Windows 10 OS. The experiment begins with a relatively small scale-free network with 20 nodes. Fig. 4 shows the results of applying these two algorithms for different k. It is observed that the convex relaxation method always provides a relatively better optimality performance than the submodular greedy algorithm, about 10% improvement in the case of $k = 20$. Furthermore, compared to the convex relaxation method, the greedy algorithm achieves a substantial reduction in computation time, about 95% decrease in the case of $k = 20$. Since the computation time of the convex relaxation method is still acceptable, about 15s in the case of $k = 20$, the convex relaxation method is preferable to the submodular greedy algorthm for relatively small scale netowrks.

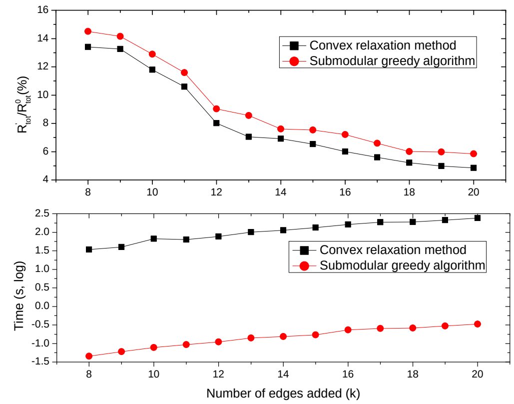

Fig. 4. The comparison of performance and running time between step by step rounding technique and submodular greedy algorithm

However, the computation time of the convex relaxation method grows exponentially as n increases as shown in Fig. 5. It becomes computationally intractable on a regular workstation for $n \geq 70$. Only the submodular greedy algorithm can be applied for large-scale netowrks. For large-scale netowrks, we compare the computation time between the basic submodular greedy algorithm and the accelerated one. Both algorithms are applied to a scale-free network with n nodes and select fixed k edges in each case. Fig. 6 shows the computation time of these two algorithms for various network sizes. It can be easily observed that the accelerated submodular greedy algorithm demonstrates a much more promising computational efficiency than the basic one. For example, the accelerated algorithm exhibits a factor of 20 speed-up in the case of $n = 150$, and it's able to optimize the networks with up to thousands nodes in hours, with nearly millions of potential edges, which is far beyond the capability of convex relaxation methods.

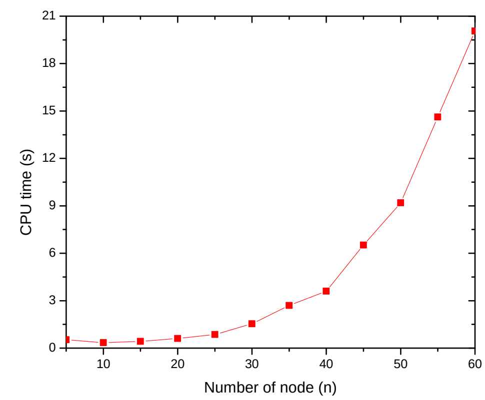

Fig. 5. CPU Time in solving a convex relaxation problem for n-node graph

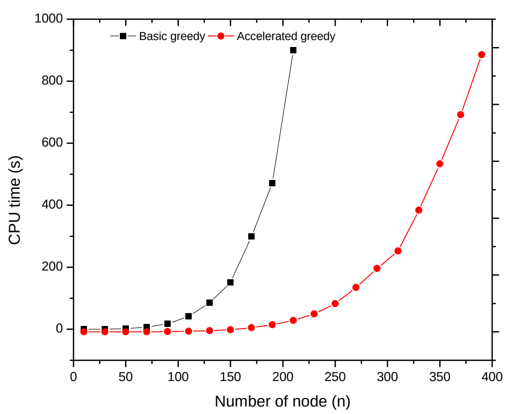

Fig. 6. The comparison of running time between basic greedy algorithm and accelerated greedy algorithm

B. Small-scale Case Study: Drone Cargo Network

A drone cargo network is studied to illustrate the application of convex relaxation with step by step rounding technique. The network changes constantly and its topology is crucial to the successful cargo delivery. The case study is about a drone cargo network of S.F. Express, one of the largest logistic companies in China. Since the drone cargo network is still under development, the network scale is relatively small so far. There are a total of 50 drones in the fleet and about 32 sorties are made every two hours in the daytime in the preliminary operation phase. The convex relaxation algorithm can achieve a better optimality performance within acceptable time. The diameter of the network is approximately 50 km and the flight distance of current electric drone is limited by 30 km. It is necessary to set up transfer airports to provide batteries for drone to extend its flight distance. Fig. 7 shows the topology of the network. Besides the delivery function of each airport, different functional characteristics are associated with airports. The star is the warehouse that stores all the goods to be delivered, the square denotes the transfer airport, and the circle denotes the final delivery airport. Batteries are backed up in the transfer airports to provide the power for drones. Setting up routes between each airport pair is impossible due to budget constraints. Besides getting the approval of flight routes from the Aviation Bureau, the telecommunication, antennae, and emergency area should also be built and associated with each route.

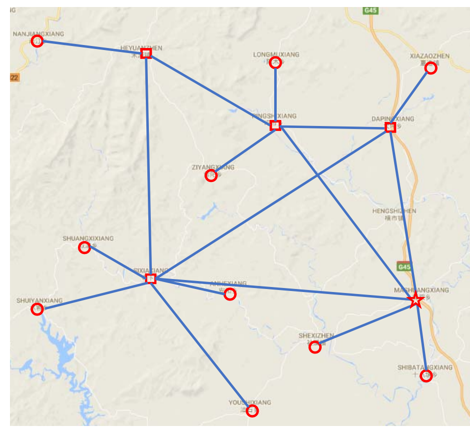

Fig. 7. S.F. Express Drone Cargo Network.

Since the drone cargo network is still under test and route failure rate data are not available, we cannot use the mechanism of mapping cancellation rates into different weights. Instead, we define the edge weight based on node degree commonly used to characterize the node centrality [54]. Generally speaking, the more routes the airport connects, the more important the airport is. Since more advanced equipments are usually equipped along the routes between critical hubs to facilitate a high demand, the routes connecting critical hubs with a higher node degree are less likely to fail, which implies a larger route weight. Therefore, we define the weight of route (i, j) as $w_{i,j} = f\left(\deg(v_i) + \deg(v_j)\right)$, where the function $f(\cdot)$ maps the sum of degree connectivity into weights $\{1,2,3\}$ based on a piecewise linear approximation.

In this case study, the convex relaxation method is applied to add $k = 5$ and $k = 10$ routes. For the case of $k = 5$, the computation time is 5.2s and the total effective resistance can be improved by 38%. The total number of acyclic paths between all node pairs can be increased from 286 to 1726. For the case of $k = 10$, the computation time is 13.6s and the total effective resistance can be improved by 60%. The total number of acyclic paths between all node pairs can be increased from 286 to 5296. Table II shows the selected routes and their associated weights in this two scenarios. It is noted that the distance of candidate routes is less than 30 km which is the drone's maximum flight duration. In a small added route set, edges tend to connect the low-degree airport and transfer airport. For example, the degree of the airports NanJiang, ZiYang, and LongMu is 1. Namely, only one route exists between each of these airports and others. If the route fails, drone cannot fly to the transfer airport by any routes or their combinations. With the increase of available route set, edges with higher weights slowly begin to connect the airports with high node degree.

TABLE II
TOP 5 AND 10 ROUTES TO BE ADDED TO S.F. DRONE CARGO NETWORK

Top 5 <route, weight>	Top 10 <route, weight>	
<NanJiang-SiXia, 3>	<NanJiang-SiXia, 3>	<YouShi-PingShi, 2>
<SiXia-ZiYang,3>	<SiXia-ZiYang, 3>	<SiXia-SheXi, 3>
<SiXia-LongMu, 3 >	<SiXia-LongMu, 3>	<HeYuang-PingShi, 2>
<SiXia-SheXi, 3>	<ShuangXi-PingShi, 2>	<HeYuang-DaPing, 2>
<SiXia-ShiBaTang, 3>	<AnHe-PingShi, 2>	<SiXia-ShiBaTang, 3>

TABLE III
TOP 5 AND 10 ROUTES TO BE ADDED TO S.F. AIR CARGO NETWORK

Top 5 <route, weight>	Top 10 <route, weight>	
<LHW-CKG, 2>	<WUH-CKG, 2>	<CKG-CGO, 2>
<CKG-WUH,2>	<LHW-CKG, 3>	<URC-KWE, 2>
<URC-KWE, 2 >	<URC-NKG, 2>	<CKG-SZX, 2>
<CKG-SZX, 2>	<CKG-PEK, 2>	<YNT-FOC, 2>
<URC-PVG, 2>	<CKG-DLC, 2>	<URC-PVG, 2>

C. Medium-scale Case Study: S.F. Airline

Although S.F. Express owns the largest cargo airline in China, its network is still in medium size [55]. There are a total of 42 cargo aircraft in the fleet and about 126 operational flights are made every day in the current operational practice. The cargo network includes 40 airports and 114 bidirectional routes as shown in Fig. 8. The existing edges are weighted based on the failure rate computed from real operations. According to the data, the flight cancellation rate ranges from 0% to 9.6%. The existing edges with cancellation rates in $[0, 3.2\%)$ are assigned a weight of 3, the ones with cancellation rates in $[3.2\%, 6.4\%)$ are assigned a weight of 2, and the ones with cancellation rates in $[6.4\%, 9.6\%]$ are assigned a weight of 1. The mechanism of mapping cancellation rates into different weights is motivated by the practical operations in the aviation industry. A flight route with a small weight indicates that it is prone to failure under disruptive situations, such as aircraft shortage or severe weather, and vice versa.

In this case study, the accelerated submodular greedy method is applied to add $k = 5$ and $k = 10$ routes, which is programmed using the same environment as described in the previous subsection. The results are illustrated in Table III with each edge name and its associated weight. For the case of $k = 5$, the computation time is 1.2s and the total effective resistance can be improved by 3.3%. For the case of $k = 10$, the computation time is 2.6s and the total effective resistance can be improved by 4.5%. Even though the network size is medium, since computing the total number of acyclic paths between all node pairs, Q, requires an exponential time complexity, it is computationally intractable to derive the exact values of Q and will be omitted for both of the medium and large-scale networks. It is noted the selected edges with weight 2 account for a large proportion, indicating those edges with medium strength are influential for the robustness improvement of overall robustness.

Fig. 8. S.F. Express Air Cargo Network

D. Large-scale Case Study: Worldwide Network

In this section, we study the application of the greedy algorithm for the worldwide air transportation network. The worldwide network supports the traffic of over three billion passengers traveling between more than 4000 airports on more than 50 million flights in a year. Since the majority of the air transportation network is based on hub-and-spoke network configuration, it is more beneficial and useful for the air transportation industry to improve the robustness of the network composed of critical hubs [56]. Based on the data for 2012 travel year from OpenFlights Database that contains 36203 routes between 3425 airports [4], 300 critical airports are selected in terms of node degree in the worldwide network as shown in Fig. 9. There are 6736 routes existing in the current network of these 300 critical airports. The accelerated submodular greedy algorithm is used to choose k routes from 38114 candidate routes between these 300 airports. The result is illustrated in Fig. 10, where the left y-axis is the relative R_{tot} defined as $R_{\text{tot}}(E_s)/R_{\text{tot}}(E_0)$. It can be observed that the computational time linearly increases and the network robustness measured by R_{tot} is continuously improved as k grows. When it reaches $k = 35$, the computation time is 2644s and the total effective resistance can be improved by 8.6%. Compared to the accelerated submodular greedy algorithm, another two heuristic methods, that is, random addition strategy and smallest node degree addition strategy that always greedily selects edges between node pair with smallest node degree, can only improve the total effective resistance by 0.61% and 1.55% respectively.

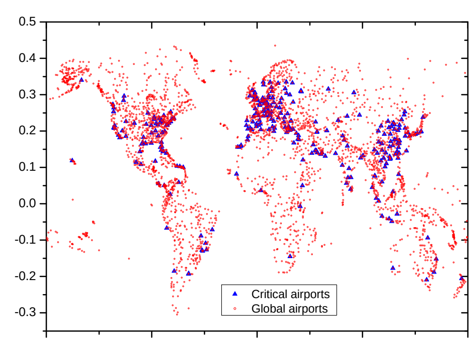

Fig. 9. 300 Critical Airports of Worldwide Air Transportation Network

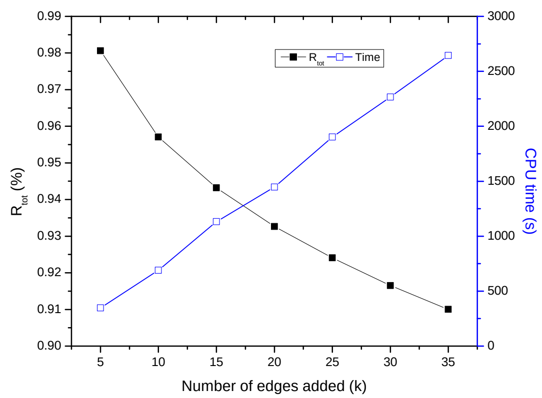

Fig. 10. Relative R_{tot} and CPU time vs the number of edges added (k) for the 300 critical hubs of the worldwide air transportation network

VII. Conclusion

In this paper, we show that the total effective resistance is a promising measure that can capture the global network characteristics and distinguish the changes of an individual node or edge. The flight route selection problem via the minimization of the total effective resistance is formulated, which is a difficult integer nonlinear programming problem. Two methods are developed for different network scales to balance the trade-off between optimality performance and computational efficiency. For small/medium-scale networks with less than 70 nodes, we develop an interior-point method based on convex relaxation and duality gap, which can achieve a near optimality within an acceptable computation time. For large-scale networks with up to thousands of airports, we develop an accelerated submodular greedy algorithm based on proved monotone submodularity, which can obtain a good solution with a guaranteed optimality gap in substantially reduced computation time. Three case studies from real practice have been conducted to demonstrate the application and performance of the proposed methods for the air transportation networks with small, medium and large scales.

The developed methods are able to enhance the robustness of air transportation networks for different levels of organizations and provide quantitative results for the decision makers. The network planners (route map planners) in airline companies are able to optimize the network. The aviation authorities, such as FAA in US and ATMB (Air Traffic Management Bureau) in China, can also evaluate a regional or national air transportation network, then restructure the airway network and give their suggestions to airline companies. The methods are also applicable for edge deletion when the airlines intend to cut down their operating budgets and try to sustain their robustness to the largest extent. The developed methods may also be used to improve the design of other networks, such as urban networks, supply chain networks, communication networks and so on. For the future work, we will pursue network optimization considering fuel efficiency [57], vulnerability [58], and network reliability [59]; other optimization strategies including edge rewiring, weights assignment, and the combination of edge addition and weight assignment will also be considered. Moreover, under some uncertain environments, even though an edge is selected, the edge may not be successfully added into the existing network and it will be more meaningful to consider the minimization of the expected total effective resistance.

References

[1] R. Guimera and L. A. N. Amaral, "Modeling the world-wide airport network," *The European Physical Journal B-Condensed Matter and Complex Systems*, vol. 38, no. 2, pp. 381–385, 2004.

[2] G. Bagler, "Analysis of the airport network of india as a complex weighted network," *Physica A: Statistical Mechanics and its Applications*, vol. 387, no. 12, pp. 2972–2980, 2008.

[3] K.-Q. Cai, J. Zhang, M.-M. Xiao, K. Tang, and W.-B. Du, "Simultaneous optimization of airspace congestion and flight delay in air traffic network flow management," *IEEE Transactions on Intelligent Transportation Systems*, 2017.

[4] [Online]. Available: http://openflights.org.

[5] [Online]. Available: https://www.transtats.bts.gov.

[6] M. T. Gudmundsson, R. Pedersen, K. Vogfjörd, B. Thorbjarnardóttir, S. Jakobsdóttir, and M. J. Roberts, "Eruptions of eyjafjallajökull volcano, iceland," *Eos, Transactions American Geophysical Union*, vol. 91, no. 21, pp. 190–191, 2010.

[7] R. Albert, H. Jeong, and A.-L. Barabási, "Error and attack tolerance of complex networks," *Nature*, vol. 406, no. 6794, pp. 378–382, 2000.

[8] J. Wu, M. Barahona, Y.-J. Tan, and H.-Z. Deng, "Spectral measure of structural robustness in complex networks," *IEEE Transactions on Systems, Man, and Cybernetics-Part A: Systems and Humans*, vol. 41, no. 6, pp. 1244–1252, 2011.

[9] I. Linkov, T. Bridges, F. Creutzig, J. Decker, C. Fox-Lent, W. Kröger, J. H. Lambert, A. Levermann, B. Montreuil, J. Nathwani *et al.*, "Changing the resilience paradigm," *Nature Climate Change*, vol. 4, no. 6, pp. 407–409, 2014.

[10] D. DeLaurentis, E.-P. Han, and T. Kotegawa, "Network-theoretic approach for analyzing connectivity in air transportation networks," *Journal of Aircraft*, vol. 45, no. 5, pp. 1669–1679, 2008.

[11] O. Lordan, J. M. Sallan, P. Simo, and D. Gonzalez-Prieto, "Robustness of the air transport network," *Transportation Research Part E: Logistics and Transportation Review*, vol. 68, pp. 155–163, 2014.

[12] ——, "Robustness of airline alliance route networks," *Communications in Nonlinear Science and Numerical Simulation*, vol. 22, no. 1, pp. 587–595, 2015.

[13] K. L. Clark, U. Bhatia, E. A. Kodra, and A. R. Ganguly, "Resilience of the us national airspace system airport network," *IEEE Transactions on Intelligent Transportation Systems*, 2018, to appear.

[14] C. Yang, "Robustness comparison experiments," *CUHKSZ Technical Report*, 2018, see also https://drive.google.com/file/d/1c8Au3F5wMqrl3jmCMD9BYb3BTT706AX5/view.

[15] P. Wei, L. Chen, and D. Sun, "Algebraic connectivity maximization of an air transportation network: The flight routes' addition/deletion problem," *Transportation Research Part E: Logistics and Transportation Review*, vol. 61, pp. 13–27, 2014.

[16] P. Wei, G. Spiers, and D. Sun, "Algebraic connectivity maximization for air transportation networks," *IEEE Transactions on Intelligent Transportation Systems*, vol. 15, no. 2, pp. 685–698, 2014.

[17] A. Ghosh, S. Boyd, and A. Saberi, "Minimizing effective resistance of a graph," *SIAM review*, vol. 50, no. 1, pp. 37–66, 2008.

[18] D. J. Klein and M. Randić, "Resistance distance," *Journal of Mathematical Chemistry*, vol. 12, no. 1, pp. 81–95, 1993.

[19] X. Wang, E. Pournaras, R. E. Kooij, and P. Van Mieghem, "Improving robustness of complex networks via the effective graph resistance," *The European Physical Journal B*, vol. 87, no. 9, pp. 1–12, 2014.

[20] J. M. Kleinberg, "Navigation in a small world," *Nature*, vol. 406, no. 6798, pp. 845–845, 2000.

[21] A.-L. Barabási *et al.*, "Scale-free networks: a decade and beyond," *science*, vol. 325, no. 5939, p. 412, 2009.

[22] R. Guimera, S. Mossa, A. Turtschi, and L. N. Amaral, "The worldwide air transportation network: Anomalous centrality, community structure, and cities' global roles," *Proceedings of the National Academy of Sciences*, vol. 102, no. 22, pp. 7794–7799, 2005.

[23] P. A. Bonnefoy, "Scalability of the air transportation system and development of multi-airport systems: A worldwide perspective," Ph.D. dissertation, Massachusetts Institute of Technology, 2008.

[24] P. A. Bonnefoy and R. J. Hansman, "Potential impacts of very light jets in the national airspace system," *Journal of aircraft*, vol. 44, no. 4, pp. 1318–1326, 2007.

[25] T. Kotegawa, D. DeLaurentis, K. Noonan, and J. Post, "Impact of commercial airline network evolution on the us air transportation system," in *Ninth USA/Europe Air Traffic Management Research and Development Seminar (ATM2011), Berlin, Germany*, 2011.

[26] M. Azzam, U. Klingauf, and A. Zock, "The accelerated growth of the worldwide air transportation network," *The European Physical Journal Special Topics*, vol. 215, no. 1, pp. 35–48, 2013.

[27] X. Sun, S. Wandelt, and F. Linke, "Temporal evolution analysis of the european air transportation system: air navigation route network and airport network," *Transportmetrica B: Transport Dynamics*, pp. 1–16, 2014.

[28] X. Sun and S. Wandelt, "Network similarity analysis of air navigation route systems," *Transportation Research Part E: Logistics and Transportation Review*, vol. 70, pp. 416–434, 2014.

[29] A. Reggiani, P. Nijkamp, and A. Cento, "Connectivity and concentration in airline networks: a complexity analysis of Lufthansa's network," *European Journal of Information Systems*, vol. 19, no. 4, pp. 449–461, 2010.

[30] D. R. Wuellner, S. Roy, and R. M. D'Souza, "Resilience and rewiring of the passenger airline networks in the united states," *Physical Review E*, vol. 82, no. 5, p. 056101, 2010.

[31] K. Cai, J. Zhang, C. Zhou, X. Cao, and K. Tang, "Using computational intelligence for large scale air route networks design," *Applied Soft Computing*, vol. 12, no. 9, pp. 2790–2800, 2012.

[32] C. Hong, J. Zhang, X.-B. Cao, and W.-B. Du, "Structural properties of the chinese air transportation multilayer network," *Chaos, Solitons & Fractals*, vol. 86, pp. 28–34, 2016.

[33] S. B. Amor and M. Bui, "A complex system approach in modeling airspace congestion dynamics," *Journal of Air Transport Studies*, vol. 3, no. 1, pp. 39–56, 2012.

[34] S. Conway, "Systemic analysis approaches for air transportation," 2005.

[35] C. M. Schneider, A. A. Moreira, J. S. Andrade, S. Havlin, and H. J. Herrmann, "Mitigation of malicious attacks on networks," *Proceedings of the National Academy of Sciences*, vol. 108, no. 10, pp. 3838–3841, 2011.

[36] V. Latora and M. Marchiori, "Efficient behavior of small-world networks," *arXiv preprint cond-mat/0101396*.

[37] E. Vargo, R. Kincaid, and N. Alexandrov, "Towards optimal transport networks," *Systemics, Cybernetics and Informatics*, vol. 8, no. 4, pp. 59–64, 2010.

[38] P. Van Mieghem, X. Ge, P. Schumm, S. Trajanovski, and H. Wang, "Spectral graph analysis of modularity and assortativity," *Physical Review E*, vol. 82, no. 5, p. 056113, 2010.

[39] W. Ellens, F. Spieksma, P. Van Mieghem, A. Jamakovic, and R. Kooij, "Effective graph resistance," *Linear algebra and its applications*, vol. 435, no. 10, pp. 2491–2506, 2011.

[40] Z.-Y. Jiang, M.-G. Liang, and D.-C. Guo, "Improving network transport efficiency by edge rewiring," *Modern Physics Letters B*, vol. 27, no. 08, 2013.

[41] A. Sydney, C. Scoglio, and D. Gruenbacher, "Optimizing algebraic connectivity by edge rewiring," *Applied Mathematics and computation*, vol. 219, no. 10, pp. 5465–5479, 2013.

[42] Z. Jiang, M. Liang, and D. Guo, "Enhancing network performance by edge addition," *International Journal of Modern Physics C*, vol. 22, no. 11, pp. 1211–1226, 2011.

[43] S. Joshi and S. Boyd, "Sensor selection via convex optimization," *IEEE Transactions on Signal Processing*, vol. 57, no. 2, pp. 451–462, 2009.

[44] J. F. Sturm, "SeDuMi," *MATLAB toolbox, May*, 1998.

[45] S. Boyd and L. Vandenberghe, *Convex optimization*. Cambridge university press, 2004.

[46] L. Lovász, "Submodular functions and convexity," in *Mathematical Programming The State of the Art*. Springer, 1983, pp. 235–257.

[47] M.-Y. Liu, O. Tuzel, S. Ramalingam, and R. Chellappa, "Entropy-rate clustering: Cluster analysis via maximizing a submodular function subject to a matroid constraint," *IEEE Transactions on Pattern Analysis and Machine Intelligence*, vol. 36, no. 1, pp. 99–112, 2014.

[48] C. Ortiz-Astorquiza, I. Contreras, and G. Laporte, "Multi-level facility location as the maximization of a submodular set function," *European Journal of Operational Research*, 2015.

[49] M. Habibi and A. Popescu-Belis, "Keyword extraction and clustering for document recommendation in conversations," *IEEE/ACM Transactions on Audio, Speech, and Language Processing*, vol. 23, no. 4, pp. 746–759, 2015.

[50] M. J. D. Powell, "Restart procedures for the conjugate gradient method," *Mathematical programming*, vol. 12, no. 1, pp. 241–254, 1977.

[51] J. Sherman and W. J. Morrison, "Adjustment of an inverse matrix corresponding to a change in one element of a given matrix," *The Annals of Mathematical Statistics*, pp. 124–127, 1950.

[52] T. Summers, I. Shames, J. Lygeros, and F. Dörfler, "Topology design for optimal network coherence," in *Control Conference (ECC), 2015 European*. IEEE, 2015, pp. 575–580.

[53] F. Dorfler and F. Bullo, "Kron reduction of graphs with applications to electrical networks," *IEEE Transactions on Circuits and Systems I: Regular Papers*, vol. 60, no. 1, pp. 150–163, 2013.

[54] O. Younis, M. Krunz, and S. Ramasubramanian, "Node clustering in wireless sensor networks: recent developments and deployment challenges," *Network, IEEE*, vol. 20, no. 3, pp. 20–25, 2006.

[55] http://www.sf-airlines.com, 2017.

[56] T. Aykin, "Lagrangian relaxation based approaches to capacitated hub-and-spoke network design problem," *European Journal of Operational Research*, vol. 79, no. 3, pp. 501–523, 1994.

[57] M. Azzam, P. Bonnefoy, and R. J. Hansman, "Investigation of the fuel efficiency of the us air transportation network structure," *Proceedings of the 10th AIAA Aviation Technology, Integration, and Operations*, 2010.

[58] Z. Wang, A. P. Chan, J. Yuan, B. Xia, M. Skitmore, and Q. Li, "Recent advances in modeling the vulnerability of transportation networks," *Journal of infrastructure systems*, vol. 21, no. 2, p. 06014002, 2014.

[59] A. Soltani-Sobh, K. Heaslip, A. Stevanovic, J. El Khoury, and Z. Song, "Evaluation of transportation network reliability during unexpected events with multiple uncertainties," *International journal of disaster risk reduction*, vol. 17, pp. 128–136, 2016.

[60] G. L. Nemhauser, L. A. Wolsey, and M. L. Fisher, "An analysis of approximations for maximizing submodular set functions-i," *Mathematical Programming*, vol. 14, no. 1, pp. 265–294, 1978.

Changpeng Yang received the B.S. degree in Aerospace Engineering in 2011 from Northwestern Polytechnical University, Xi'an, China, the M.S. degree in Control Science and Engineering in 2014 from Shanghai Jiao Tong University. He received his Ph.D. degree in ATMRI of Nanyang Technological University, Singapore. He was also affiliated with NEXTOR II in the University of California, Berkeley, USA. He is now working in SF express as a senior operations researcher. His research interests include network optimization, machine learning, and reinforcement learning.

Jianfeng Mao received the B.E. degree and M.E. degree in Automation Science from Tsinghua University, Beijing, China in 2001 and 2004 respectively, and Ph.D. degree in Systems Engineering from Boston University, Boston, MA, U.S. in 2009. From 2010 to 2016, he was a Faculty Member with the School of Mechanical and Aerospace Engineering, Nanyang Technological University, Singapore. He is currently an assistant professor with the School of Science and Engineering, the Chinese University of Hong Kong, Shenzhen, China. He specializes in the areas of modeling and optimization of discrete event and hybrid systems with applications to transportation systems, smart grid, computer networks, sensor networks and healthcare systems. He is the recipient of several awards, including the best conference paper award of 2017 IEEE Conference on Automation Science and Engineering, the 2017 Shenzhen Overseas High-level Talents Peacock Plan Type B Award, the best paper award of 2012 Industrial and Systems Engineering Research Conference, and the 2009 Best PhD Dissertation Award Finalist of Boston University College of Engineering. He is an associate editor of the journal of Discrete Event Dynamic Systems: Theory and Applications from 2013. He serves on several program committees of international conferences.

Xiongwen Qian received his Bachelor of Engineering in Automation from Shanghai Jiao Tong University in 2009. He continued his study as a dual-master program student and was conferred Master of Engineering in Control Theory and Control Engineering and Master of Science in Industrial Engineering, from Shanghai Jiao Tong University and Georgia Institute of Technology, respectively, in 2012. He is currently pursuing his Ph.D., at the School of Mechanical and Aerospace Engineering, Nanyang Technological University, in the field of Air Traffic Management and Airline Operations.

Peng Wei is an assistant professor in Iowa State University Aerospace Engineering Department, with courtesy appointments in Electrical and Computer Engineering Department and Computer Science Department. He is also an affiliated faculty member with the FAA Center of Excellence for General Aviation (PEGASAS), and the Human Computer Interaction graduate program at Virtual Reality Applications Center (VRAC) at ISU. Prof. Wei is leading the Intelligent Aerospace Systems Lab (IASL). With methods from control, optimization, machine learning, and artificial intelligence, he develops autonomous and decision making systems for: Air Traffic Control/Management (ATC/M), Airline Operations, UAS Traffic Management (UTM), and eVTOL Urban Air Mobility (UAM). Prof. Wei received his undergraduate degree in Information Science and Control Theory from Tsinghua University in 2007, a master degree in Electrical and Computer Engineering from Stony Brook University in 2009, and a Ph.D. degree in Aerospace Engineering from Purdue University in 2013.

VIII. Appendix

A. Proof of Theorem 1

Proof. The convexity property can be proved by verifying that the Hessian matrix of R_{tot} is positive semidefinite. To prove the property, we need to introduce the following identity function(see [45], section A.4.1), $\frac{\partial X^{-1}}{\partial t} = -X^{-1}\frac{\partial X}{\partial t}X^{-1}$, where invertible symmetric matrix $X(t)$ is a differentiable function of the parameter $t \in \mathbf{R}$. Define $\bar{L}(y) = L(y) + \mathbf{1}\mathbf{1}^T/n$ and $h_{e,w} = w_e^{\frac{1}{2}} h_e$, we can express the gradient as

$$\begin{aligned}
\frac{\partial R_{\text{tot}}}{\partial y_e} &= -n\mathbf{tr}[\bar{L}(y)^{-1}\frac{\partial \bar{L}(y)}{\partial y_e}\bar{L}(y)^{-1}] \\
&= -n\mathbf{tr}[\bar{L}(y)^{-1}\frac{\partial(\bar{L}_0 + \sum_e y_e h_{e,w} h_{e,w}^T)}{\partial y_e}\bar{L}(y)^{-1}] \\
&= -n\mathbf{tr}[\bar{L}(y)^{-1} h_{e,w} h_{e,w}^T \bar{L}(y)^{-1}] \\
&= -n\|(\bar{L}(y))^{-1} h_{e,w}\|^2.
\end{aligned}$$

where $\|\cdot\|$ denotes the Frobenius norm, we have $\partial R_{\text{tot}}/\partial y_e \leq 0$, thus $R_{\text{tot}}(L(y))$ is a nonincreasing function of y, indicating a larger value of y leads to a better network in terms of R_{tot}.

Let $A_w = [h_{1,w} \cdots h_{p,w}]$, we can express the gradient as

$$\nabla R_{\text{tot}} = -n\text{diag}(A_w^T(\bar{L}_E(y))^{-2}A_w)$$

We now derive the Hessian matrix of $R_{\text{tot}}(y)$ from the derivative matrix,

$$\begin{aligned}
\frac{\partial^2 R_{\text{tot}}}{\partial y_e \partial y_k} &= -n\frac{\partial}{\partial y_k}\|(\bar{L}_E(y))^{-1}h_{e,w}\|^2 \\
&= 2nh_{e,w}^T(\bar{L}_E(y))^{-2}h_{k,w}h_{k,w}^T(\bar{L}_E(y))^{-1}h_{e,w}
\end{aligned}$$

Using the definition of A_w, we can express the Hessian of $R_{\text{tot}}(y)$ as

$$\nabla^2 R_{\text{tot}} = 2n(A_w^T(\bar{L}_E(y))^{-2}A_w) \circ (A_w^T(\bar{L}_E(y))^{-1}A_w) \succeq 0$$

where $\circ$ denotes the Hadamard product. The inequality above can be established because both the first component and second component of the product matrix are positive semidefinite. $\square$

B. Proof of Theorem 2

Proof. The solution $S = (\Lambda, \mu, \nu)$ is evidently feasible for the dual problem, so its dual objective value gives a lower bound $\underline{R}$ on $R_{\text{tot}}(y)$, $\underline{R} \leq R_{\text{tot}}(y)$

$$\begin{aligned}
\underline{R} &= 2\mathbf{tr}(n\Lambda)^{1/2} - (1/n)\mathbf{1}\Lambda\mathbf{1}^T - \nu k - \mathbf{tr}(\Lambda L_0) - \mathbf{1}^T\mu - n \\
&= 2n\mathbf{tr}(L + \mathbf{1}\mathbf{1}^T/n)^{-1} - \|(L + \mathbf{1}\mathbf{1}^T/n)^{-1}\mathbf{1}\|^2 - \mathbf{tr}(\Lambda L_0) \\
&\quad - \max_e nk\|(L + \mathbf{1}\mathbf{1}^T/n)^{-1}h_e\|^2 - n \\
&= 2n\mathbf{tr}(L + \mathbf{1}\mathbf{1}^T/n)^{-1} - n\mathbf{tr}((L + \mathbf{1}\mathbf{1}^T/n)^{-2}L_0) - 2n \\
&\quad - \max_e nk\|(L + \mathbf{1}\mathbf{1}^T/n)^{-1}h_e\|^2.
\end{aligned}$$

In the second line, we use $(L + \mathbf{1}\mathbf{1}^T/n)^{-1}\mathbf{1} = \mathbf{1}$. Let δ denote the difference between this lower bound $\underline{R}$ and the value of R_{tot} achieved by the selected edge vector y. There is a duality gap associated with y, using $R_{\text{tot}} =$

$n\mathbf{tr}(L+\mathbf{1}\mathbf{1}^T/n)^{-1}-n$, the gap δ between the lower bound $\underline{R}$ and the value of R_{tot} can be expressed as,

$$\begin{aligned}\delta &= R_{\text{tot}}(y)-\underline{R}\\ &= -n\mathbf{tr}(L+\mathbf{1}\mathbf{1}^T/n)^{-1}+\max_e nk\|(L+\mathbf{1}\mathbf{1}^T/n)^{-1}h_e\|^2\\ &\quad + n\mathbf{tr}(L_0(L+\mathbf{1}\mathbf{1}^T/n)^{-2})+n\\ &= -\max_e(kw_e^{-1}\frac{\partial R_{\text{tot}}}{\partial y_e})+n\mathbf{tr}(L_0(L+\mathbf{1}\mathbf{1}^T/n)^{-2})-R_{\text{tot}}\\ &= -\max_e(R_{\text{tot}}-n\mathbf{tr}(L_0(L+\mathbf{1}\mathbf{1}^T/n)^{-2})+kw_e^{-1}\frac{\partial R_{\text{tot}}}{\partial y_e})\end{aligned}$$

□

C. Proof of Theorem 3

Proof. Taking any $A\subseteq B\subseteq E_P$ and $e\in E_P\setminus B$, we have

$$\begin{aligned}&f(A\cup\{e\})-f(A)=-R_{\text{tot}}(L_{A\cup E_0}+L_e)+R_{\text{tot}}(L_{A\cup E_0})\\ &=-n\mathbf{tr}(L_{A\cup E_0}+L_e+\mathbf{1}\mathbf{1}^T/n)^{-1}+n\mathbf{tr}(L_{A\cup E_0}+\mathbf{1}\mathbf{1}^T/n)^{-1}\\ &=-n\mathbf{tr}[(L_{A\cup E_0}+L_e+\mathbf{1}\mathbf{1}^T/n)^{-1}-(L_{A\cup E_0}+\mathbf{1}\mathbf{1}^T/n)^{-1}]\\ &=n\mathbf{tr}\left[\frac{L_e}{(L_{A\cup E_0}+\mathbf{1}\mathbf{1}^T/n)(L_{A\cup E_0}+L_e+\mathbf{1}\mathbf{1}^T/n)}\right]\\ &\geq n\mathbf{tr}\left[\frac{L_e}{(L_{B\cup E_0}+\mathbf{1}\mathbf{1}^T/n)(L_{B\cup E_0}+L_e+\mathbf{1}\mathbf{1}^T/n)}\right]\\ &=-n\mathbf{tr}[(L_{B\cup E_0}+L_e+\mathbf{1}\mathbf{1}^T/n)^{-1}-(L_{B\cup E_0}+\mathbf{1}\mathbf{1}^T/n)^{-1}]\\ &=f(B\cup\{e\})-f(B)\end{aligned}$$

where the inequality satisfies since $L_{A\cup E_0}\preceq L_{B\cup E_0}$ and thus $(L_{A\cup E_0}+\mathbf{1}\mathbf{1}^T/n)^{-1}\succeq(L_{B\cup E_0}+\mathbf{1}\mathbf{1}^T/n)^{-1}$, $(L_{A\cup E_0}+L_e+\mathbf{1}\mathbf{1}^T/n)^{-1}\succeq(L_{B\cup E_0}+L_e+\mathbf{1}\mathbf{1}^T/n)^{-1}$. Therefore, we have

$$f(A\cup\{e\})-f(A)\geq f(B\cup\{e\})-f(B) \tag{12}$$

which implies that the set function $f(E)$ is submodular. It can be easily shown that $f(E)$ is also monotone increasing. Hence, $f(E)$ is a monotone submodular function. □

D. Proof of Theorem 4

Proof. Let f^{OPT} be the value of an optimal solution to problem (10) and f^G be the value of a particular solution to (10). There exists a greedy algorithm which begins with empty set, $S\leftarrow\varnothing$ and computes the loss $\Delta(e|S_i)=f(e|S_i)-f(S_i)$ for all elements $e\in E$ till the kth iteration. In each step, the algorithm selects the element with the highest loss

$$S_{i+1}\leftarrow S_i\cup\{\arg\max_e\Delta(e|S_i)|e\in E\}.$$

As shown in [60], if f is a monotone increasing and submodular function, then the greedy algorithm always produces a solution satisfying

$$\frac{f^{\text{OPT}}-f^G}{f^{\text{OPT}}-f(\varnothing)}\leq(\frac{k-1}{k})^k\leq\frac{1}{e}$$

Combining it with Theorem 3, the greedy algorithm in Algorithm 3 results in

$$\frac{-R_{\text{tot}}^{\text{OPT}}+R_{\text{tot}}^{\text{G}}}{-R_{\text{tot}}^{\text{OPT}}+R_{\text{tot}}(E_0)}\leq\frac{1}{e} \tag{13}$$

where E_0 is the existing edges of the initial network. Rearranging the inequality (13), we have

$$\begin{aligned}R_{\text{tot}}^{\text{G}}&\leq\frac{1}{e}R_{\text{tot}}(E_0)+(1-\frac{1}{e})R_{\text{tot}}^{\text{OPT}}\\ &=(\frac{R_{\text{tot}}(E_0)}{eR_{\text{tot}}^{\text{OPT}}}+1-\frac{1}{e})R_{\text{tot}}^{\text{OPT}}\\ &\leq(\frac{R_{\text{tot}}(E_0)}{eR_{\text{tot}}^{*}}+1-\frac{1}{e})R_{\text{tot}}^{\text{OPT}}\\ &=(1+\frac{\alpha-1}{e})R_{\text{tot}}^{\text{OPT}}\end{aligned}$$

The second inequality is satisfied because $R_{\text{tot}}^{*}\leq R_{\text{tot}}^{\text{OPT}}$ and R_{tot}^{*} is the optimal value obtained by adding all the candidate edges with given weights. □

E. Proof of Theorem 5

Proof. Define $\overline{L}_E=L_E+\mathbf{1}\mathbf{1}^T/n$ and $h_{e,w}=w_e^{\frac{1}{2}}h_e$, it holds that

$$\begin{aligned}R_{\text{tot}}(E\cup e)&=n\mathbf{tr}(L_{E\cup e}+\mathbf{1}\mathbf{1}^T/n)^{-1}-n\\ &=n\mathbf{tr}(L_E+\mathbf{1}\mathbf{1}^T/n+w_eh_eh_e^T)^{-1}-n\\ &=n\mathbf{tr}(\bar{L}_E+h_{e,w}h_{e,w}^T)^{-1}-n\end{aligned} \tag{14}$$

Since the rank of L_E+11^T/n is n and invertible, $\beta=1+w_eh_e^T(L_E+\mathbf{1}\mathbf{1}^T/n)^{-1}h_e>0$. From the Sherman-Morrison formula [51], we have

$$\left(\overline{L}_E+h_{e,w}h_{e,w}^T\right)^{-1}=\overline{L}_E^{-1}-\frac{1}{\beta}\overline{L}_E^{-1}h_{e,w}h_{e,w}^T\overline{L}_E^{-1}$$

Using the equality above, we can reformulate equation (14) as

$$\begin{aligned}R_{\text{tot}}(E\cup e)&=n\mathbf{tr}(\bar{L}_E+h_{e,w}h_{e,w}^T)^{-1}-n\\ &=n\mathbf{tr}(\overline{L}_E^{-1}-\frac{1}{\beta}\overline{L}_E^{-1}h_{e,w}h_{e,w}^T\overline{L}_E^{-1})-n\\ &=n\mathbf{tr}(\overline{L}_E^{-1})-n-\frac{n}{\beta}\mathbf{tr}(\overline{L}_E^{-1}h_{e,w}h_{e,w}^T\overline{L}_E^{-1})\\ &=R_{\text{tot}}(E)-\frac{n}{\beta}\|\overline{L}_E^{-1}h_{e,w}\|^2\\ &=R_{\text{tot}}(E)-\frac{nw_e}{\beta}\|(L_E+11^T/n)^{-1}h_e\|^2\end{aligned} \tag{15}$$

which implies (11). □